BIOCHEMISTRY
including biophysical chemistry & molecular biology

Article

pubs.acs.org/biochemistry

NMR Structure of Calmodulin Complexed to an N-Terminally Acetylated α-Synuclein Peptide

James M. Gruschus,*[,†] Thai Leong Yap,[†] Sara Pistolesi,[†] Alexander S. Maltsev,[‡] and Jennifer C. Lee*[,†]

[†]Laboratory of Molecular Biophysics, Biochemistry and Biophysics Center, National Heart, Lung, and Blood Institute, National Institutes of Health, Bethesda, Maryland 20892, United States

[‡]Laboratory of Chemical Physics, National Institute of Diabetes and Digestive and Kidney Diseases, National Institutes of Health, Bethesda, Maryland 20892, United States

ABSTRACT: Calmodulin (CaM) is a calcium binding protein that plays numerous roles in Ca-dependent cellular processes, including uptake and release of neurotransmitters in neurons. α-Synuclein (α-syn), one of the most abundant proteins in central nervous system neurons, helps maintain presynaptic vesicles containing neurotransmitters and moderates their Ca-dependent release into the synapse. Ca-Bound CaM interacts with α-syn most strongly at its N-terminus. The N-terminal region of α-syn is important for membrane binding; thus, CaM could modulate membrane association of α-syn in a Ca-dependent manner. In contrast, Ca-free CaM has negligible interaction. The interaction with CaM leads to significant signal broadening in both CaM and α-syn NMR spectra, most likely due to conformational exchange. The broadening is much reduced when binding a peptide consisting of the first 19 residues of α-syn. In neurons, most α-syn is acetylated at the N-terminus, and acetylation leads to a 10-fold increase in binding strength for the α-syn peptide (K_D = 35 ± 10 μM). The N-terminally acetylated peptide adopts a helical structure at the N-terminus with the acetyl group contacting the N-terminal domain of CaM and with less ordered helical structure toward the C-terminus of the peptide contacting the CaM C-terminal domain. Comparison with known structures shows that the CaM/α-syn complex most closely resembles Ca-bound CaM in a complex with an IQ motif peptide. However, a search comparing the α-syn peptide sequence with known CaM targets, including IQ motifs, found no homologies; thus, the N-terminal α-syn CaM binding site appears to be a novel CaM target sequence.

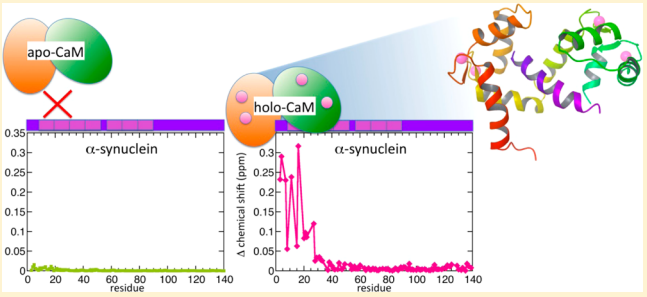

The protein α-synuclein (α-syn) is well known for its association with Parkinson's disease, a neurodegenerative disease involving the loss of dopamine-producing neurons.[1,2] The histological hallmark of the disease is the presence of Lewy bodies, proteinaceous inclusions found in the neurons of Parkinson's patients.[3] α-Syn is a primary constituent of Lewy bodies,[4] and though the majority of Parkinson's cases have no clear genetic cause,[5] rare mutations in α-syn as well as gene duplication and triplication lead to an autosomal dominant form of the disease.[6−9] A vertebrate specific protein, α-syn is expressed primarily in neurons of the central nervous system (CNS).[10] It is found at the highest concentrations (∼100 μM) in the presynaptic spaces at the ends of axons.[11] Lower levels of the protein are observed in other cell types of the CNS, and the gene is also transcribed in other tissues, such as the heart, skeletal muscle, and pancreas.[10]

Despite extensive study, pinpointing specific biological roles for α-syn has proven difficult. Mice with the α-syn gene (*SNCA*) knocked out presented no obvious pathology, with only subtle perturbation of neuronal function.[12] There are two other α-syn-related proteins expressed in neurons, β-syn, expressed primarily in the CNS, and γ-syn, expressed mostly in peripheral neurons. Mice with both α-syn and β-syn knocked out likewise displayed only subtle CNS changes.[13] However, for mice with all three synuclein genes knocked out, pathology was pronounced, altering synaptic structure and transmission and causing age-dependent neuronal dysfunction, implying a role for the synucleins in long-term maintenance of neurons.[14] Detailed investigation of neurotransmitter release from presynaptic vesicles has revealed a role for α-syn as a chaperone protein, aiding the rapid reassembly of the SNARE complex of proteins.[15] The SNARE complex is responsible for membrane fusion in the exocytosis process that releases the neurotransmitters from the vesicles into the synapse.[16]

Neurotransmitter release is a carefully regulated event, where the voltage pulse of the firing neuron traveling down the axon introduces calcium into the presynaptic space via voltage-gated calcium channels.[17] The neuron has numerous proteins that bind calcium, many of which act as calcium-sensitive triggers of various signaling pathways.[18,19] One of the most important calcium-binding proteins is calmodulin (CaM), ubiquitously expressed in all cell types, regulating processes throughout the cell from the cell membrane to the nucleus.[20] Binding calcium

Received: February 15, 2013
Revised: April 22, 2013
Published: April 22, 2013

dx.doi.org/10.1021/bi400199p | *Biochemistry* 2013, 52, 3436−3445

induces structural changes in CaM that target it to bind peptide sequences in numerous proteins.[21] While CaM does not directly induce neurotransmitter release, this role belongs to another calcium-binding protein, synaptotagmin,[19] it regulates the exocytosis process in multiple ways, for instance, via its interactions with calcium-CaM-dependent kinase II.[22] At higher concentrations CaM can inhibit SNARE-mediated membrane fusion.[23] CaM regulates exocytosis in other secretory cell types too, such as adrenal chromaffin cells and pancreatic β-cells,[24,25] where α-syn is also expressed and affects the release of secretory vesicles.[26,27]

Three studies have reported interaction between α-syn and CaM.[28−30] Given the association of these proteins with presynaptic and other secretory vesicles, an interaction between the two has important implications regarding how CaM might regulate secretory processes. The two earlier studies reported binding affinities in the submicromolar range,[28,29] more than strong enough to allow interaction in neurons, where both α-syn and CaM can reach concentrations in the 10−100 μM range.[11,19] However, the later study observed a much weaker dissociation constant, ∼10 μM, and questioned the physiological relevance of the interaction.[30]

These studies showed that the N-terminal region of α-syn interacts with CaM. It is now known that the protein is N-terminally acetylated;[31,32] however, the previous studies on CaM interaction were done with nonacetylated α-syn. In addition, two of the studies reached different conclusions regarding the role of calcium in the interaction, with one report seeing interaction only in the presence of calcium-bound (holo-) CaM, whereas the other observed little difference between the two forms. Understanding the difference between apo- and holo-CaM binding to α-syn is critical for gaining insight into how this interaction might regulate calcium-triggered secretion.

Here, we examined the binding of α-syn to CaM using nuclear magnetic resonance (NMR) spectroscopy in both its N-terminally acetylated (Ac-α-syn) and nonacetylated forms with both apo- and holo-CaM. By monitoring changes in the NMR spectra due to interaction, we map the interacting regions in α-syn and CaM at the residue level. Using an N-terminally acetylated peptide containing the first 19 residues (AcN19) of α-syn, we determine the 3-dimensional solution structure of the CaM/α-syn peptide complex.

MATERIALS AND METHODS

Protein and Peptide Expression and Purification. Full-length nonacetylated α-syn was expressed in *E. coli* and purified as previously described.[33,34] N-Terminally acetylated, full-length α-syn was obtained by coexpression in *E. coli* of a plasmid carrying the components of the NatB complex[35] with a plasmid containing the wild-type α-syn gene followed by a C-terminal His-tag sequence and purification as described in Maltsev et al.[36]

Natural abundance α-syn N-terminal peptides N19 (MDVFMKGLSKAKEGVVAAA-NH_2) and the N-terminally acetylated form AcN19 (Ac-MDVFMKGLSKAKEGVVAAA-NH_2) were purchased from Biosynthesis (Lewisville, TX). Isotopically labeled AcN19 peptide (Ac-MDVFMKGLSKAK-EGVVAAA-NH_2), where underlined residues are uniformly $^{13}C/^{15}N$-labeled, was purchased from Anaspec (Fremont, CA). Peptide amounts were determined gravimetrically, and concentrations were confirmed by 1-D NMR comparison with standards.

Human CaM was expressed using a pET17b plasmid in *E. coli* BL21(DE3) pLysS and purified by ammonium sulfate precipitation, anionic exchange chromatography on a DEAE column, and Ca-dependent hydrophobic interaction chromatography on a phenyl sepharose column. Ammonium sulfate precipitation was done using 52 g of ammonium sulfate per 100 mL lysate solution after centrifugation removing cellular debris (20 mM Tris, 200 mM NaCl, and 1 mM EDTA at pH 8). The precipitated pellet was resuspended in and dialyzed against 20 mM Tris and 1 mM EDTA at pH 8 buffer. The sample was then applied to a DEAE column (GE Healthcare) and eluted using a linear NaCl gradient from 0.05 to 1.0 M. Pooled fractions were applied to a phenyl sepharose column after the additions of $(NH_4)_2SO_4$ (1 M) and $CaCl_2$ (5 mM) and eluted with a linear gradient from 20 mM HEPES, 1 M $(NH_4)_2SO_4$, and 5 mM $CaCl_2$ at pH 7.5 to 20 mM HEPES and 5 mM EDTA at pH 7.5. To prepare apo-CaM, the protein was passed through a column containing chelex resin (200−400 mesh, Biorad) equilibrated with 50 mM $(NH_4)HCO_3$ at pH 9.0. All NMR samples were exchanged into a buffer containing 50 mM MES, 100 mM NaCl, and 3 mM $CaCl_2$ at pH 6.4, except for samples with apo-CaM where $CaCl_2$ was omitted, and with 5% D_2O.

NMR Spectroscopy. Experiments were carried out on Bruker Avance 600, 800, and 900 MHz spectrometers equipped with cryoprobes. Backbone resonance assignment of the $^{13}C/^{15}N$-labeled holo-CaM, free and bound to natural abundance α-syn, full-length, and peptides AcN19 and N19 was done by standard techniques at 600 MHz using CBCA(CO)NH and HNCACB experiments at 300 K. Resonance assignment for full-length α-syn, free and bound, was done similarly. Resonance assignment of the isotopically labeled AcN19, both free and in complex with CaM, was done by ^{15}N-edited NOESY (800 MHz, t_{mix} = 500 ms for free and 100 ms for the complex). ^{15}N-edited NOESY (800 MHz, t_{mix} = 100 ms), aliphatic ^{13}C-edited NOESY (900 MHz, t_{mix} = 100 ms, ^{13}C frequency = 40 ppm) and aromatic ^{13}C-edited NOESY (800 MHz, t_{mix} = 100 ms, ^{13}C frequency = 125 ppm) spectra were measured for structure determination for $^{13}C/^{15}N$-labeled CaM in complex with natural abundance AcN19 and for isotopically labeled AcN19 in complex with natural abundance CaM. Chemical shift perturbations for the titration analyses were obtained from ^{15}N heteronuclear single-quantum correlation (HSQC) spectra at 800 MHz. To confirm sufficient calcium was present to form fully calcium bound holo-CaM, the ^{15}N HSQC spectrum of CaM in complex with N19 peptide was also recorded with 5 mM $CaCl_2$, and no perturbations were seen compared to the spectrum with 3 mM $CaCl_2$.

Backbone HN-N residual dipolar couplings (RDCs) were measured for CaM using in-phase/antiphase HSQC measured at 800 and 900 MHz in filamentous phage pf1 (10 mg/mL). Backbone HN-N and Hα-Cα residual dipolar couplings were also measured at 800 MHz using ^{15}N and ^{13}C HSQC with no ^{1}H decoupling during indirect evolution. The squared deviation from average in the three measured amide RDC values in phage was summed, divided by two (not three since the true average is not known), and the square root taken, yielding an experimental uncertainty of 0.72 Hz. When combined with the r.m.s deviation of the isotropic j-coupling values measured in two separate experiments, 0.25 Hz, this yielded a total uncertainty of 0.76 Hz for the amide RDC values. The T_2 relaxation and ^{15}N CPMG chemical exchange rates were

dx.doi.org/10.1021/bi400199p | *Biochemistry* 2013, 52, 3436−3445

measured by standard procedures.[37] Except where noted above, all experiments were done at 310 K. All spectra were processed with NMRPipe.[38]

Titration binding curves were fit to the two-state binding model (AB ↔ A + B), with species A being titrated at concentration a into solution with species B held at constant concentration b using the following equation:

$$\Delta(a) = (\Delta_{max}/2b)(a + K_D + b - \sqrt{(a + K_D + b)^2 - 4ab})$$

where $\Delta(a)$ is the measured chemical shift perturbation of species B at concentration a of species A. The two fit parameters are K_D, the dissociation constant, and Δ_{max}, the asymptotic limit of the chemical shift perturbation. To simultaneously fit several residues, one residue was arbitrarily chosen, and the rest were scaled by a factor

$$f_i = \sum \Delta_0(a)\Delta_i(a) / \sum \Delta_i^2(a)$$

where $\Delta_0(a)$ is the perturbation at concentration a of the residue to scale, and $\Delta_i(a)$ is the perturbation of the residue to be scaled, and the sums are carried out over all concentrations. Following the determination of Δ_{max} in the fit, the vertical scale of the plot was divided by Δ_{max} to give percent saturation. All fits were performed using Kaleidagraph (Synergy Software).

K_D of the N19 peptide was estimated assuming that values of Δ_{max} for the CaM backbone amides were similar to those determined in the titration binding curves using AcN19. Then, in the fast NMR time scale regime, the fraction bound is equal to $\Delta(a)/\Delta_{max}$, and the fraction unbound is $(1-\Delta(a)/\Delta_{max})$ in the 1:1 complex, where $\Delta(a)$ is the perturbation measured at concentration a. Then K_D is simply

$$K_D = \frac{[A][B]}{[AB]} = a\frac{\Delta_{max}}{\Delta(a)}\left(1 - \frac{\Delta(a)}{\Delta_{max}}\right)^2$$

K_D values were estimated this way for 10 different amides in the CaM complex, with their standard deviation given as the error.

In the backbone HN chemical shift perturbation versus residue plots, the combined HN perturbation was calculated as

$$\Delta_{HN} = \sqrt{\frac{1}{2}\left(\Delta_H^2 + \frac{\Delta_N^2}{5}\right)}$$

where Δ_H and Δ_N are the differences in the proton and the nitrogen frequencies in ppm, respectively.

Structure Determination. Backbone dihedral phi and psi restraints were obtained using TALOS+[39] based on the observed Cα, Cβ, Hα, and N frequencies using only dihedrals predicted with high confidence, with ranges equal to twice the TALOS+ uncertainty. NOE-derived distance restraints were obtained for assigned NOE cross-peaks, using peak intensities (heights) normalized by the corresponding diagonal peak intensities. Normalized intensities from the CaM NOESY spectra were converted to distances by calibrating with a subset of nonoverlapped cross-peaks arising from close intra, sequential, and medium range distances in regions of well-defined covalent and secondary structure, yielding $d(Å) = 1.82 \cdot I^{(-0.222)}$ for the ^{15}N-edited NOESY, $d(Å) = 1.67 \cdot I^{(-0.190)}$ for the aliphatic ^{13}C-edited NOESY, and $d(Å) = 2.34 \cdot I^{(-0.212)}$ for the aromatic ^{13}C-edited NOESY where d is distance, and I is the normalized cross-peak intensity. Upper and lower bounds were determined by assuming a factor of 10 variability in intensity. As the NOESY spectra from the labeled peptide had too few appropriate cross-peaks for calibration, peptide distance restraints used the same formulas as calibrated for CaM. Four calcium ions were placed at the known binding sites[40] and restrained to be within 2.2−2.6 Å of their four respective monodentate coordinated carboxyl and carboxylate oxygens, and within 2.3−2.7 Å of the carboxylate oxygens of the bidentate coordinated glutamates.

Structures were calculated by simulated annealing using the XPLOR-NIH program.[41] For the RDC restraints, the average value of the measured HN-N residual dipolar couplings and Hα-Cα residual dipolar couplings were used. RDC restraints were included for all residues whose RDC values could be measured accurately, with no spectral overlap, with the exception of residues with large measured ^{15}N chemical exchange rates and those residues adjacent to them. Alignment tensor parameters were first calculated with XPLOR-NIH using only the RDC restraints for the CaM N-terminal domain (D_A, −5.0; rhombicity, 0.67) and then only those for the C-terminal domain (D_A, −5.0; rhombicity, 0.60). The average D_A and rhombicity values were used as starting values and their values optimized during the structure calculations. Floating chirality was employed for diastereotopic methylene and methyl groups.[42] One hundred structures were generated, with a high starting temperature 10,000 K to allow thorough sampling for floating chiral groups. For backbone and side chain dihedral angles, the torsionDBPot term in XPLOR-NIH was employed.[43] The radius of gyration for CaM structures, i.e., the r.m.s. distance from the centroid of the protein structure, was calculated using all CaM coordinates, including both heavy and hydrogen atoms.

RESULTS

Spectra of CaM Bound to Full-Length α-Syn and N-Terminal Peptides. NMR spectra of the holo-CaM complexes with α-syn and Ac-α-syn were recorded, including spectra with isotopically labeled CaM and spectra with isotopically labeled α-syn and Ac-α-syn. In the ^{15}N HSQC spectra of CaM bound to either form of α-syn, all CaM backbone amide resonances except for the first two residues were observed, similar to the free form. However, many CaM resonances were significantly broadened in the complex (Figure 1a), indicating significant environmental fluctuations at those amide positions, possibly due to (1) local motions induced by binding, (2) exchange between different bound forms of CaM, or (3) exchange between bound and unbound forms.

In the ^{15}N HSQC spectra of α-syn and Ac-α-syn, the largest chemical shift perturbations due to holo-CaM interaction are seen in the stretch spanning the first 20 residues with additional, smaller perturbations for residues 20−30 (Figure 2a). Half of the backbone amides in this N-terminal region disappeared, presumably due to broadening. The Cα and Cβ resonances for the first 29 α-syn residues also disappeared in the spectra of the complex, while the Cα and Cβ resonances for residues 30−140 were the same as free α-syn within error. Negligible perturbations were seen with apo-CaM, calmodulin with no bound calcium (Figure 2a).

Since CaM typically binds to a helical segment of approximately 20 amino acids,[44] we recorded spectra for complexes with isotopically labeled CaM using N-terminally acetylated (AcN19) and nonacetylated (N19) peptides consisting of the first 19 amino acids of α-syn. These first 19 residues were chosen for study because they not only show the largest perturbations but also include the first of seven

dx.doi.org/10.1021/bi400199p | Biochemistry 2013, 52, 3436−3445

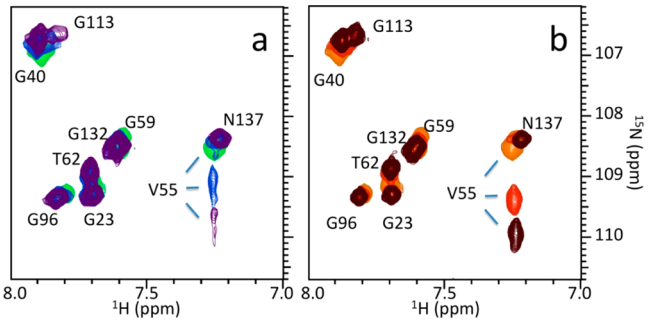

Figure 1. Reduction in holo-CaM NMR resonance broadening when bound to N-terminally acetylated α-syn peptide (AcN19) compared to acetylated, full-length α-syn (Ac-α-syn). (a) The ^{15}N HSQC spectra of a selected region of 100 μM holo-CaM with 0 μM (green), 50 μM (blue), and 100 μM (purple) of Ac-α-syn are superimposed. Significant broadening is seen for the Val 55 amide signal in the ^{15}N dimension, and broadening of the Gly 113 amide signal is also apparent. (b) Spectra of the same region of 100 μM holo-CaM with 0 μM (orange), 50 μM (red), and 100 μM (brown) of AcN19 are superimposed. The signals for Val 55 and Gly 113 are much stronger, a consequence of much less broadening when interacting with the peptide.

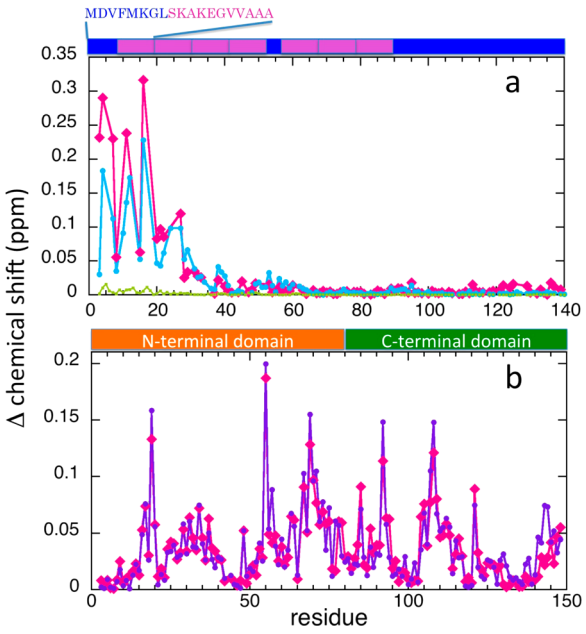

Figure 2. α-Syn and CaM backbone amide chemical shift perturbations upon CaM/α-syn interaction, with primary sequence diagrams shown above. (a) The first 100 residues of α-syn contain 7 imperfect repeats of 11 residues each (purple rectangles), and the α-syn AcN19 peptide sequence shown above contains the first of these repeats (purple lettering). Backbone amide chemical shift perturbations as a function of residue for 100 μM Ac-α-syn (red diamonds) and nonacetylated α-syn (blue circles) in the presence of 100 μM holo-CaM, and in the presence of 100 μM apo-CaM (green squares). (b) CaM consists of two lobes, the N-terminal domain (orange, residues 1−79) and the C-terminal domain (green, residues 80−148). Backbone amide chemical shift perturbations for 100 μM holo-CaM in the presence of 100 μM α-syn AcN19 peptide (violet circles) and 100 μM Ac-α-syn (red diamonds).

imperfect 11 amino acid amphiphatic helix repeat (^{9}XKXKEGVXXXX^{19}) motifs in the N-terminal region (Figure 2a). Stronger signals with less broadening were observed for the peptide compared to full-length α-syn (Figure 1b) with quite similar chemical shift perturbations for the most part (Figure 2b). Closer inspection of the perturbations in Figure 2b, however, reveals differences in the C-terminal region CaM, suggesting that these residues might be affected by portions of α-syn near or beyond residue 19.

Binding Strengths of CaM/α-Syn Complexes. The strength of binding of α-syn to CaM was estimated by titrating increasing amounts of unlabeled α-syn, with constant CaM concentration, and fitting the chemical shift perturbations of CaM resonances to a two-state binding equilibrium. This procedure is valid when bound and free forms exchange on the fast NMR time scale, typically faster than 10 ns, though the exact number depends on a number of factors, including magnitude of chemical shift change between forms, and thus can vary from residue to residue.[45] NMR resonance broadening occurs when local environmental fluctuations become slower than the fast time scale; thus, care was taken to choose resonances with no significant broadening. The perturbations of each residue were scaled as described in Materials and Methods to allow a global fit. The global fits for Ac-α-syn and the corresponding peptide, AcN19, are shown in Figure 3a.

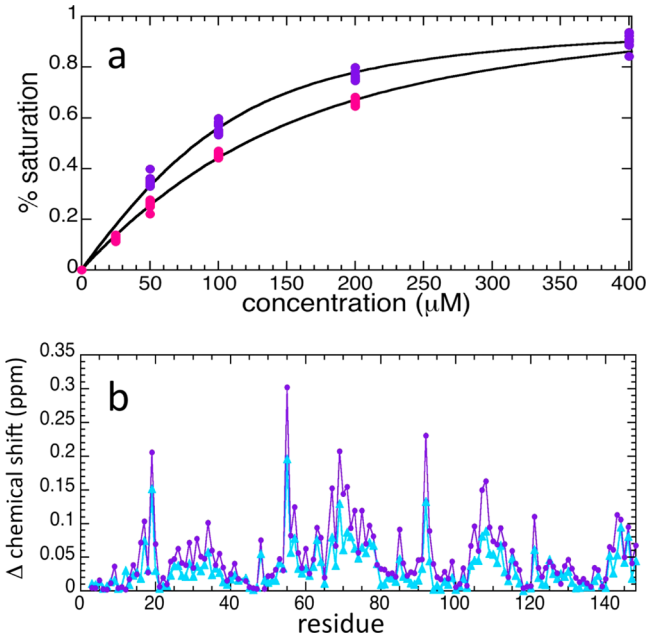

Figure 3. Binding data to determine dissociation constants for Ac-α-syn and AcN19 and comparison of holo-CaM perturbations due to AcN19 and nonacetylated α-syn peptide, N19. (a) Global fits of chemical shift perturbations for 10 selected backbone amide resonances of holo-CaM (100 μM), due to the titration of AcN19 peptide (purple) and Ac-α-syn (pink), scaled on the y-axis to correspond to the fraction of holo-CaM bound. The black curves are fits to a two-state, one-to-one binding equilibrium. (b) Backbone amide chemical shift perturbations of holo-CaM in a 1:1 complex with AcN19, protein and peptide both at 600 μM (violet circles), and with N19, protein and peptide both at 900 μM (blue triangles).

AcN19 appears to bind twice as strongly to CaM (K_D = 35 ± 10 μM) compared to Ac-α-syn (K_D = 70 ± 20 μM). The titration for full-length α-syn was not extended to 400 μM due to limited material; nevertheless, sufficient data are present to fit the binding curve, albeit with greater uncertainty. The resulting dissociation constants are consistent with Figure 2b, where slightly larger chemical shift perturbations of CaM are

dx.doi.org/10.1021/bi400199p | Biochemistry 2013, 52, 3436−3445

seen when bound to the peptide, with α-syn peptide or protein and CaM all at 100 μM.

A very similar pattern of changes in the CaM spectra was observed for CaM/AcN19 versus CaM/N19 but with the ^{1}H and ^{15}N chemical shift perturbations scaled down by a constant factor in the CaM/N19 complex (Figure 3b). Assuming that the asymptotic limits of the chemical shift changes for both acetylated and nonacetylated forms are similar at saturating concentrations of the respective peptides, our data would indicate that the binding constant for the nonacetylated peptide is at least 10 times weaker than that for the acetylated peptide, estimated as 540 $\pm$ 200 μM (see Materials and Methods).

T_2 Relaxation and CPMG Dispersion of CaM. In order to further assess molecular motions associated with resonance broadening, T_2 relaxation and CPMG dispersion experiments were performed on CaM bound to AcN19 (Figure 4). CaM

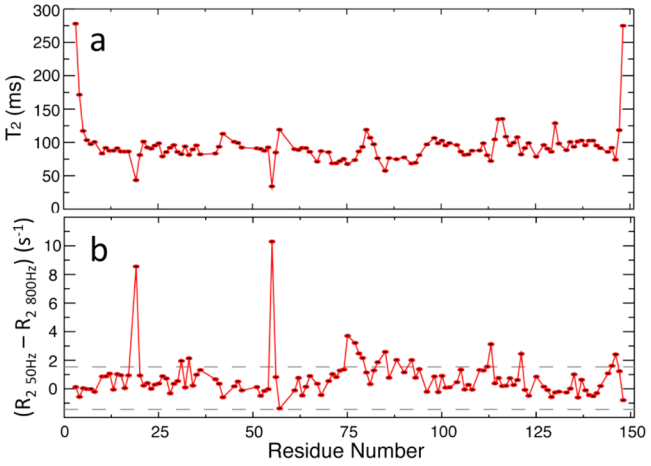

Figure 4. Backbone dynamics of holo-CaM in the complex with AcN19. (a) Transverse backbone ^{15}N relaxation times (T_2) and (b) CPMG dispersion chemical exchange rates (R_{ex}), taking the difference in transverse relaxation rates measured at 50 and 800 Hz repetition rate of the CPMG refocusing pulse train, and with the noise threshold indicated by dashed lines. The concentrations of CaM and AcN19 were 600 μM.

consists of two lobes, the N- (residues 1−79) and C- (residues 80−148)-terminal domains (Figure 2b), and both domains show similar backbone ^{15}N T_2 times on average, indicating that they experience similar overall molecular tumbling in the complex. The amide ^{15}N chemical exchange rates calculated from the CPMG dispersion experiment show two CaM N-terminal domain residues with large rates, Phe 19 and Val 55, indicating that the N-terminal domain experiences significant fluctuations in its environment in the bound form on the millisecond time scale.

Secondary Structure of the AcN19 Peptide. To test whether using the α-syn peptide would also reduce broadening of the α-syn resonances, a ^{15}N HSQC spectrum was recorded of unlabeled CaM in complex with a ^{13}C/^{15}N-labeled AcN19 peptide. CaM−peptide complexes involve numerous hydrophobic contacts,[44] and due to the greater cost of isotopically labeled hydrophilic residues, only hydrophobic residues in the peptide were labeled with ^{13}C and ^{15}N. Also, because α-syn is found predominantly in the N-terminally acetylated form *in vivo*,[31,32] we chose not to study the isotopically labeled, nonacetylated peptide. Figure 5 shows the AcN19 peptide ^{15}N HSQC spectra for free and CaM-bound forms. Significant

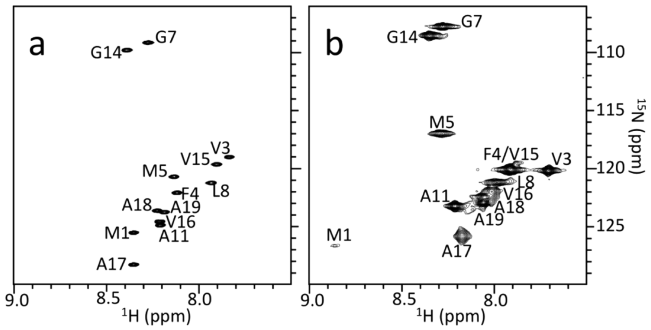

Figure 5. ^{15}N HSQC spectra of (a) isotopically labeled α-syn AcN19 peptide free in solution and (b) bound in a 1:1 complex with holo-CaM, with protein and peptide concentrations of 700 μM.

broadening is still present in the bound form, but six residues not previously observed for full-length α-syn are now seen, including the acetylated first residue, Met 1.

Backbone amides and side chains of the isotopically labeled α-syn peptide were assigned by standard techniques, and additional backbone proton assignments for nonlabeled residues were deduced via NOE cross-peaks in ^{15}N-edited and ^{13}C-edited NOESY spectra. A summary of the secondary structure for the bound peptide is shown in Figure 6, along with

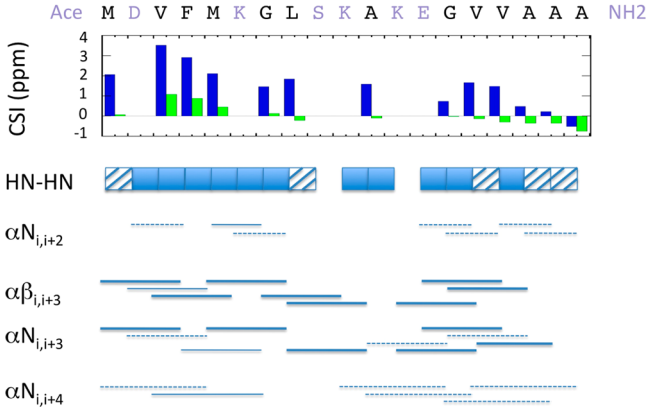

Figure 6. Summary of holo-CaM-bound AcN19 peptide α-helical secondary structure data. The peptide sequence is shown on top, with nonisotopically labeled residues in gray. The $\Delta C\alpha-\Delta C\beta$ chemical shift index (CSI) is shown in the histogram below the sequence for bound AcN19 (blue) and free AcN19 (green). Positive CSI values correlate with more helical structure. Observed NOE cross-peaks for the complex are indicated below, with solid squares and lines indicating observed nonambiguous cross-peaks. Hatched squares and dashed lines indicate where the expected peaks are overlapped with stronger signals and thus can neither be confirmed nor ruled out. The absence of squares and lines indicates where expected cross-peaks were not observed (for isotopically labeled residues) or could not be observed due to lack of isotopic labeling for that particular residue.

the $\Delta C\alpha-\Delta C\beta$ chemical shift indices[45] of the free peptide. Unfortunately, the Cα and Cβ resonances of these residues for bound full-length α-syn could not be observed, presumably due to the same exchange process that causes disappearance of most of the amide resonances in the same region. For the bound peptide, the chemical shift indices are largest at the N-terminus. For free AcN19, the indices near the N-terminus are still slightly positive, indicating that it may retain some degree of helical structure free in solution, confirming results from previous studies.[36,46]

dx.doi.org/10.1021/bi400199p | *Biochemistry* 2013, 52, 3436−3445

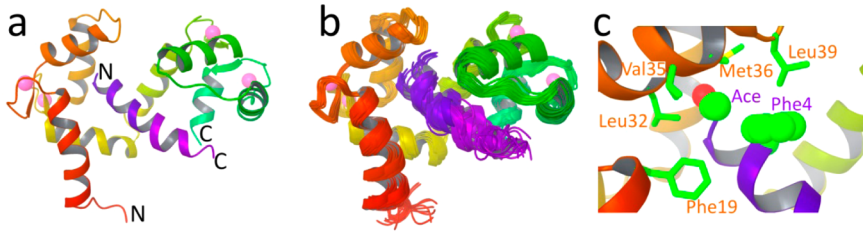

Figure 7. NMR solution structure of the holo-CaM/AcN19 complex (pdb code 2m55). (a) The lowest energy structure is shown with the CaM N-terminal domain going from red to yellow and its C-terminal domain going from yellow-green to green. The bound peptide is purple. The calcium ions are shown as pink spheres. (b) Superposition of the 20 lowest energy structures of the complex. (c) Close-up view of the N-terminal region of AcN19 (acetyl group (Ace) and Phe 4, in purple lettering) making hydrophobic contacts with the CaM N-terminal domain (residues Phe 19, Leu 32, Val 35, Met 36, and Leu 39, in orange lettering).

Solution Structure of the CaM/N-Terminally Acetylated α-Syn Peptide Complex. The improvement in the spectra using AcN19 made a full structure determination of the complex feasible (pdb code 2m55). ^{15}N-Edited, aliphatic ^{13}C-edited, and aromatic ^{13}C-edited NOESY spectra were collected for isotopically labeled CaM bound to unlabeled peptide and unlabeled CaM bound to isotopically labeled peptide yielding a total of 3451 NOE distance restraints, with 216 arising from the peptide spectra. A total of 29 nonambiguous NOE CaM-peptide cross-peaks were observed, with 21 from the peptide spectra. Using the measured backbone chemical shifts, backbone phi and psi restraints were generated with the TALOS+ program, 258 for CaM and 22 for the isotopically labeled residues of AcN19.

Two nonambiguous N- to C-terminal domain NOE cross-peaks were observed in the NOESY spectra of CaM, though 17 ambiguous cross-peaks were also observed, a consequence of the many degenerate chemical shifts at the putative interdomain interface. Many residues at the putative interface show broadened resonances, the side chain amides of Gln 41 and Asn 111, and Hα of Val 108, for example, indicating dynamics in the intermediate NMR time scale (roughly 100 ns−100 ms).[47] The implications of the dynamics observed at the interface are addressed in the discussion. To further probe the CaM interdomain orientation, residual dipolar couplings were measured for the CaM/AcN19 complex in pf1 phage, yielding 103 amide HN-N and 44 Hα-Cα RDC restraints.

One hundred structures were calculated with XPLOR-NIH, and 20 with the lowest energies were retained. The structure that best fit the restraints is shown in Figure 7a along with the superposition of the 20 structures in Figure 7b. Table 1 summarizes the r.m.s. errors in the experimental restraints and geometry, and various backbone and all-atom r.m.s. deviations of the superposed structures. The backbone r.m.s. deviation of 1.18 Å for the complex reflects the uncertainty in the positioning of the two domains of CaM, as well as the uncertainty in the bound peptide structure. Superposing each domain of CaM individually yields much smaller backbone deviations, 0.34 Å for the N-terminal and 0.57 Å the C-terminal domain. The bound α-syn peptide shows the greatest structural uncertainty, with a backbone r.m.s. deviation of 1.67 Å superposing just the peptide. Its structure is more consistently helical near its N-terminus and becomes progressively less helical toward the C-terminus, in agreement with its ΔCα−ΔCβ chemical shift indices seen in Figure 6. The N-terminal acetyl group of the peptide is packed against the CaM N-terminal domain, with Phe 4 of the peptide making numerous hydrophobic N-terminal domain contacts (Figure 7c), while the C-terminal portion of the peptide contacts the CaM C-terminal domain.

Table 1. Statistics for the NMR Structure of the Holo-CaM/AcN19 α-Syn Peptide Complex

restraints (number)	r.m.s. violation	superposition	r.m.s.d.
NOE (3451)	0.076 Å	all heavy	1.36 Å
dihedral (280)	0.48°	all backbone	1.18 Å
RDC (147)	0.74 Hz	peptide backbone	1.67 Å
geometry		CaM backbone	0.82 Å
bond	0.004 Å	CaM N-domain bb	0.34 Å
angle	0.57°	CaM C-domain bb	0.57 Å
improper	0.52°		
		Ramachandran Plot	
RDC parameters		most favored	92%
Da	−4.93 Hz	additional allowed	8%
Rh	0.65		
(HN-N) *R*-factor	10.4		
(Hα-Cα) *R*-factor	5.0		

DISCUSSION

Over 60 structures of CaM complexes with peptides have been previously determined. A Dali structural similarity search[48] using the NMR structure of the CaM complex with α-syn peptide AcN19 found many close matches, the closest being a holo-CaM complex with the IQ motif peptide of the calcium channel protein Ca(v)1.2 (pdb code 2F3Y[49]), with an r.m.s. deviation of 3.4 Å, aligning the backbones of both CaM and the bound peptides. IQ motifs are found in a variety of proteins, myosin and neuromodulin, for example, and the consensus sequence is shown in Figure 8. Both AcN19 and Ca(v)1.2 IQ motif peptides have their N-terminus packed against the N-terminal domain of CaM, but, surprisingly, there is almost no similarity in the peptide sequences. Phe 4 contributes the most hydrophobic contacts with the N-terminal domain in the CaM/α-syn complex (Figure 7c); in contrast, the IQ motif peptide

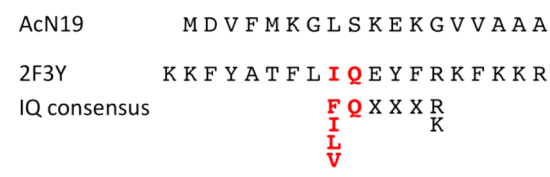

Figure 8. Alignment of the AcN19 peptide sequence with the IQ motif peptide of the cardiac Ca(v)1.2 calcium channel, pdb structure 2F3Y. The IQ portion is highlighted in red, and the consensus IQ sequence is shown below.

dx.doi.org/10.1021/bi400199p | *Biochemistry* 2013, 52, 3436−3445

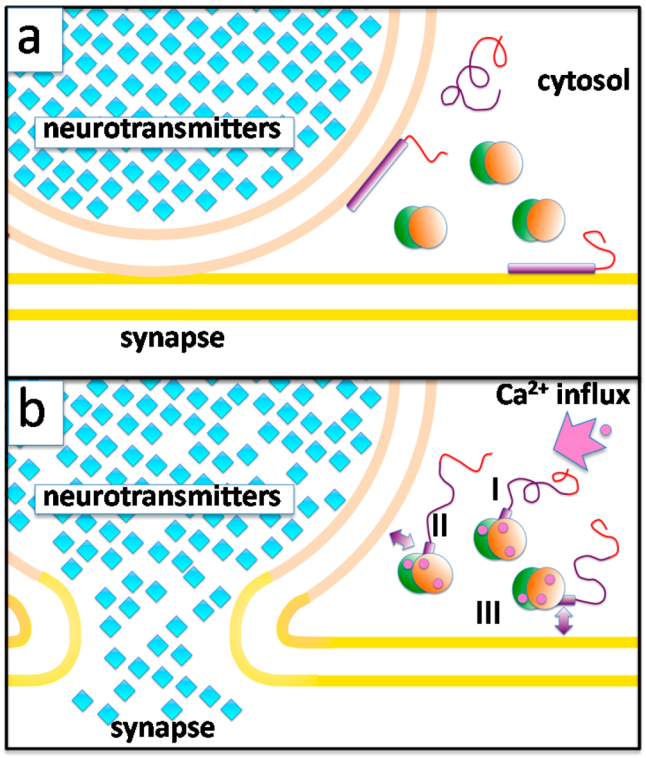

Figure 9. Diagram of hypothetical CaM/α-syn interactions in the presynaptic region of an axon, near a docked vesicle containing neurotransmitters (a) before voltage induced Ca^{2+} influx. (b) After Ca^{2+} influx, apo-CaM (with two lobes, orange and green) binds Ca^{2+} (pink dots) and can bind α-syn (purple with red C-terminal region): (I) holo-CaM interacting with cytosolic α-syn; (II and III) holo-CaM competing with the membrane for α-syn interaction.

has an alanine in this position with few protein contacts. The α-syn binding site sequence appears to be novel; a search in the Calmodulin Target Database[21] using the AcN19 peptide sequence produced no hits.

The CaM/α-syn complex is more open, that is, with fewer N- to C-terminal domain contacts than other CaM/peptide complex structures. Using pdb coordinates, calculated radii of gyration (see Materials and Methods) of CaM/peptide complexes typically fall in the 15−17 Å range, while the radius calculated from the CaM/α-syn complex coordinates is 18 Å. For example, the CaM/IQ peptide complex (2F3Y), whose structure is most similar to the CaM/α-syn peptide complex, has a radius of gyration of 16.4 Å. The more open structure is a consequence of the few observed NOE signals between the domains. To test whether the RDC restraints also contributed to the larger radius of the complex, the structure calculation was repeated without them. The resulting structures had practically the same radii but with different interdomain orientation and a much more pronounced bend in the middle of the bound peptide; thus, the RDC restraints influence domain orientation but not the radius of gyration of the complex.

The broadening of signals seen for several of the residues at the domain interface arises from dynamics in the intermediate NMR time scale, roughly in the range from 100 ns to 100 ms.[47] One possibility is that dynamics occur only locally for the affected residues without affecting overall structure. It is also plausible that exchange occurs between different domain orientations, between more closed and more open structures, for example. In the study by Bertini et al.,[30] they found that for CaM bound to full-length, nonacetylated α-syn many interdomain orientations could possibly contribute to the ensemble but that the most probable was a closed orientation similar to the structure presented here. In a later study that re-examined the same data, the CaM domain orientation in their α-syn complex is found to be similar to 2F3Y, the same structure identified by our Dali structural similarity search.[50]

CaM interaction most strongly perturbs the first 20 residues of α-syn, both for the acetylated and nonacetylated forms. This stretch of residues contains the first of 7 imperfect, 11-residue repeats in the α-syn sequence (Figure 2a). In addition, this region, in particular residues 1−15, can bind the membrane with an affinity comparable to that of the full-length protein.[51] It has been observed that CaM can compete with the membrane for α-syn binding, at least for the nonacetylated form.[28] While the peptide chosen for the structural study encompasses the region of strongest perturbations for full-length α-syn, the smaller perturbations seen for α-syn residues 20−29 could indicate additional structural features in this region. Furthermore, the structure near the C-terminus of the bound peptide, the less defined peptide helical structure, for instance, could arise due to truncation. Residues 30−140, however, have Cα and Cβ chemical shifts in the bound form indistinguishable from free α-syn and thus are predicted to be random coil.

The binding of CaM to N-terminally acetylated α-syn, (K_d = 70 ± 20 μM), is weaker than values reported in previous studies,[28−30] and much weaker than the nanomolar values typically seen for other CaM/peptide complexes.[44] However, the interaction was strengthened by 2-fold, (K_d = 35 ± 10 μM) in the case of AcN19. Perhaps CaM has some degree of unfavorable interaction with residues past the first 19. Another possibility is that CaM binding competes with intramolecular interactions between the N-terminal and other regions within α-syn. Indeed, interaction between the N- and C-terminal regions of α-syn is known to occur.[52,53] Additionally, unfavorable interaction with the C-terminal His-tag of the acetylated α-syn cannot be ruled out. The acetylated peptide binds to holo-CaM significantly more tightly than the corresponding nonacetylated peptide (K_d = 540 ± 200 μM). This is despite the fact that acetylation removes a positive charge from the N-terminus and since CaM has a net negative charge (−16, including Ca^{2+} ions), acetylation might result in less favorable electrostatic interaction. However, burial of a charged group at a hydrophobic interface incurs a desolvation penalty. In addition, acetylation increases the helical content of the α-syn N-terminal region[36,46] and should predispose it to the helical structure seen in the complex. Evidently, reduced cost of desolvation and/or helical predisposition due to acetylation compensates for less favorable electrostatics.

There is disagreement whether apo-CaM can interact with α-syn,[28,29] though in our hands no interaction was seen. The dependence on calcium suggests CaM/α-syn interaction could play a role in calcium-triggered events in neurons and other cell types where α-syn is found. α-Syn is concentrated in the presynaptic region of axons, where voltage induced Ca^{2+} influx triggers fusion of neurotransmitter-containing vesicles with the plasma membrane, releasing their cargos into the synaptic gap. Much of the α-syn in neurons resides in the cytosol,[54] and it could be in this cellular milieu where Ca^{2+} binding to CaM leads to biologically relevant interaction with α-syn. However, a significant fraction of α-syn is also membrane-bound;[54] indeed, N-terminal acetylation increases its affinity for negatively

charged membranes.[36] α-Syn binds to holo-CaM with a binding constant comparable to that of α-syn binding membranes containing anionic lipids.[55,56] Thus, competition between holo-CaM and the membrane for the binding of α-syn might play some role, perhaps facilitating the transport of α-syn from the membrane to the cytosol during Ca^{2+} influx. Intriguingly, α-syn has been proposed to stabilize the curved surface of vesicles; thus, loss of bound α-syn could conceivably aid the fusion process.[57] These hypothetical CaM/α-syn interactions are depicted in Figure 9.

In conclusion, CaM forms a complex with the N-terminal region of α-syn, the same region known to be most important for membrane binding. This interaction is dependent on Ca^{2+}, as negligible binding was seen with apo-CaM, and so could play a role in calcium-triggered events in cells where both CaM and α-syn are present. The binding constant of CaM to α-syn is quite weak, however, and it seems unlikely that α-syn binding to CaM could compete with other CaM substrates without additional factors to promote interaction. Further study is needed to determine whether the interaction of CaM with α-syn plays a significant biological role.

AUTHOR INFORMATION

Corresponding Author

*(J.M.G.) Phone: 1-301-496-2350. E-mail: gruschuj@helix.nih.gov. (J.C.L.) Phone: 1-301-496-3741. E-mail: leej4@nhlbi.nih.gov.

Funding

This work is supported by the Intramural Research Program at the National Institutes of Health (NIH), National Heart, Lung, and Blood Institute (NHLBI), and National Institute of Diabetes and Digestive and Kidney Diseases (NIDDK).

Notes

The authors declare no competing financial interest.

ACKNOWLEDGMENTS

We thank Nico Tjandra (NHLBI, NIH) for the use of the NMR spectrometers.

ABBREVIATIONS

CaM, calmodulin; syn, synuclein; NMR, nuclear magnetic resonance; r.m.s, root-mean-square; HSQC, heteronuclear single quantum correlation; NOESY, nuclear Overhauser effect spectroscopy; RDC, residual dipolar coupling; Ac, acetyl; SNARE, SNAP (soluble NSF attachment protein) receptor; Tris, tris(hydroxymethyl)aminomethane; MES, 2-(*N*-morpholino)ethanesulfonic acid; EDTA, ethylenediaminetetraacetic acid; HEPES, 4-(2-hydroxyethyl)-1-piperazineethanesulfonic acid; *E. coli*, *Escherichia coli*; N19, peptide consisting of the first 19 residues of α-synuclein; AcN19, N-terminally acetylated peptide consisting of the first 19 residues of α-synuclein; pdb, Protein Data Bank; IQ, isoleucine glutamine; Ca(v)1.2, calcium channel, voltage-dependent; L type, alpha 1C subunit; Rh, rhombicity

REFERENCES

(1) Cookson, M. R. (2009) α-Synuclein and neuronal cell death. *Mol. Neurodegener. 4*, 9.

(2) Clayton, D. F., and George, J. M. (1999) Synucleins in synaptic plasticity and neurodegenerative disorders. *J. Neurosci. Res. 58*, 120–129.

(3) Bethlem, J., and den Hartog, J. W. A. (1960) The incidence and characteristics of Lewy bodies in idiopathic paralysis agitans (Parkinson's disease). *J. Neurol. Neurosurg. Psychiat. 23*, 74–80.

(4) Gai, W. P., Yuan, H. X., Li, X. Q., Power, J. T., Blumbergs, P. C., and Jensen, P. H. (2000) *In situ* and *in vitro* study of colocalization and segregation of α-synuclein, ubiquitin, and lipids in Lewy bodies. *Exp. Neurol. 166*, 324–33.

(5) Lee, V.M.-Y., and Trojanowski, J. Q. (2006) Mechanisms of Parkinson's disease linked to pathological α-synuclein: New targets for drug discovery. *Neuron 52*, 33–38.

(6) Polymeropoulos, M. H., Lavedan, C., Leroy, E., Ide, S. E., Dehejia, A., Dutra, A., Pike, B., Root, H., Rubenstein, J., Boyer, R., Stenroos, E. S., Chandrasekharappa, S., Athanassiadou, A., Papapetropoulos, T., Johnson, W. G., Lazzarini, A. M., Duvoisin, R. C., Di Iorio, G., Golbe, L. I., and Nussbaum, R. L. (1997) Mutation in the α-synuclein gene identified in families with Parkinson's disease. *Science 276*, 2045–2047.

(7) Krüger, R., Kuhn, W., Müller, T., Woitalla, D., Graeber, M., Kösel, S., Przuntek, H., Epplen, J. T., Schöls, L., and Riess, O. (1998) Ala30Pro mutation in the gene encoding α-synuclein in Parkinson's disease. *Nat. Genet. 18*, 106–108.

(8) Chartier-Harlin, M. C., Kachergus, J., Roumier, C., Mouroux, V., Douay, X., Lincoln, S., Levecque, C., Larvor, L., Andrieux, J., Hulihan, M., Waucquier, N., Defebvre, L., Amouyel, P., Farrer, M., and Destee, A. (2004) α-Synuclein locus duplication as a cause of familial Parkinson's disease. *Lancet 364*, 1167–1169.

(9) Singleton, A. B., Farrer, M., Johnson, J., Singleton, A., Hague, S., Kachergus, J., Hulihan, M., Peuralinna, T., Dutra, A., Nussbaum, R., Lincoln, S., Crawley, A., Hanson, M., Maraganore, D., Adler, C., Cookson, M. R., Muenter, M., Baptista, M., Miller, D., Blancato, J., Hardy, J., and Gwinn-Hardy, K. (2003) α-synuclein locus triplication causes Parkinson's disease. *Science 302*, 841–841.

(10) Uéda, K., Fukushima, H., Masliah, E., Xia, Y., Iwai, A., Yoshimoto, M., Otero, D. A., Kondo, J., Ihara, Y., and Saitoh, T. (1993) Molecular cloning of cDNA encoding an unrecognized component of amyloid in Alzheimer disease. *Proc. Natl. Acad. Sci. U.S.A. 90*, 11282–11286.

(11) Iwai, A., Masliah, E., Yoshimoto, M., Ge, N., Flanagan, L., deSilva, H. A., Kittel, A., and Saitoh, T. (1995) The precursor protein of non-Aβ component of Alzheimer's disease amyloid is a presynaptic protein of the central nervous system. *Neuron 14*, 467–475.

(12) Abeliovich, A., Schmitz, Y., Fariñas, I., Choi-Lundberg, D., Ho, W. H., Castillo, P. E., Shinsky, N., Verdugo, J. M., Armanini, M., Ryan, A., Hynes, M., Phillips, H., Sulzer, D., and Rosenthal, A. (2000) Mice lacking α-synuclein display functional deficits in the nigrostriatal dopamine system. *Neuron 25*, 239–252.

(13) Chandra, S., Fornai, F., Kwon, H. B., Yazdani, U., Atasoy, D., Liu, X., Hammer, R. E., Battaglia, G., German, D. C., Castillo, P. E., and Südhof, T. C. (2004) Double-knockout mice for α- and β-synucleins: Effect on synaptic functions. *Proc. Natl. Acad. Sci. U.S.A. 101*, 14966–14971.

(14) Greten-Harrison, B., Polydoro, M., Morimoto-Tomita, M., Diao, L., Williams, A. M., Nie, E. H., Makani, S., Tian, N., Castillo, P. E., Buchman, V. L., and Chandra, S. S. (2010) αβγ-Synuclein triple knockout mice reveal age-dependent neuronal dysfunction. *Proc. Natl. Acad. Sci. U.S.A. 107*, 19573–19578.

(15) Burré, J., Sharma, M., Tsetsenis, T., Buchman, V., Etherton, M. R., and Südhof, T. C. (2010) α-Synuclein promotes SNARE-complex assembly in vivo and in vitro. *Science 329*, 1663–1667.

(16) Rizo, J., and Sudhof, T. C. (2002) Snares and Munc18 in synaptic vesicle fusion. *Nat. Rev. Neurosci. 3*, 641–653.

(17) Rusakov, D. A. (2006) Ca^{2+}-dependent mechanisms of presynaptic control at central synapses. *Neuroscientist 12*, 317–326.

(18) Berridge, M. J. (1998) Neuronal Calcium Signaling. *Neuron 21*, 13–26.

(19) McCue, H. V., Haynes, L. P., and Burgoyne, R. D. (2010) The diversity of calcium sensor proteins in the regulation of neuronal function. *Cold Spring Harb. Perspect. Biol. 2*, 8.

(20) Chin, D., and Means, A. R. (2000) Calmodulin: A prototypical calcium sensor. *Trends Cell Biol. 10*, 322−328.
(21) Yap, K. L., Kim, J., Truong, K., Sherman, M., Yuan, T., and Ikura, M. (2000) Calmodulin target database. *J. Struct Funct. Genomics 1*, 8−14.
(22) Pang, Z. P., Cao, P., Xu, W., and Südhof, T. C. (2010) Calmodulin controls synaptic strength via presynaptic activation of calmodulin kinase II. *J. Neurosci. 30*, 4132−4142.
(23) Di Giovanni, J., Iborra, C., Maulet, Y., Lévêque, C., El Far, O., and Seagar, M. (2010) Calcium-dependent regulation of SNARE-mediated membrane fusion by calmodulin. *J. Biol. Chem. 285*, 23665−23675.
(24) Palfrey, H. C., and Artalejo, C. R. (1997) Role of calmodulin as a regulator of Ca^{2+}-dependent exocytosis in adrenal chromaffin cells. *Pflugers Arch. 434*, 859−863.
(25) Epstein, P. N., Ribar, T. J., Decker, G. L., Yaney, G., and Means, A. R. (1992) Elevated beta-cell calmodulin produces a unique insulin secretory defect in transgenic mice. *Endocrinology 130*, 1387−1393.
(26) Larsen, K. E., Schmitz, Y., Troyer, M. D., Mosharov, E., Dietrich, P., Quazi, A. Z., Savalle, M., Nemani, V., Chaudhry, F. A., Edwards, R. H., Stefanis, L., and Sulzer, D. (2006) α-Synuclein overexpression in PC12 and chromaffin cells impairs catecholamine release by interfering with a late step in exocytosis. *J. Neurosci. 26*, 11915−11922.
(27) Geng, X., Lou, H., Wang, J., Li, L., Swanson, A. L., Sun, M., Beers-Stolz, D., Watkins, S., Perez, R. G., and Drain, P. (2011) α-Synuclein binds the K(ATP) channel at insulin-secretory granules and inhibits insulin secretion. *Am. J. Physiol. Endocrinol. Metab. 300*, 276−286.
(28) Lee, D., Lee, S. Y., Lee, E. N., Chang, C. S., and Paik, S. R. (2002) α-Synuclein exhibits competitive interaction between calmodulin and synthetic membranes. *J. Neurochem. 82*, 1007−1017.
(29) Martinez, J., Moeller, I., Erdjument-Bromage, H., Tempst, P., and Lauring, B. (2003) Parkinson's disease-associated α-synuclein is a calmodulin substrate. *J. Biol. Chem. 278*, 17379−17387.
(30) Bertini, I., Gupta, Y. K., Luchinat, C., Parigi, G., Peana, M., Sgheri, L., and Yuan, J. (2007) Paramagnetism-based NMR restraints provide maximum allowed probabilities for the different conformations of partially independent protein domains. *J. Am. Chem. Soc. 129*, 12786−12794.
(31) Anderson, J. P., Walker, D. E., Goldstein, J. M., de Laat, R., Banducci, K., Caccavello, R. J., Barbour, R., Huang, J. P., Kling, K., Lee, M., Diep, L., Keim, P. S., Shen, X. F., Chataway, T., Schlossmacher, M. G., Seubert, P., Schenk, D., Sinha, S., Gai, W. P., and Chilcote, T. J. (2006) Phosphorylation of Ser-129 is the dominant pathological modification of α-synuclein in familial and sporadic Lewy body disease. *J. Biol. Chem. 281*, 29739−29752.
(32) Bartels, T., Choi, J. G., and Selkoe, D. J. (2011) α-Synuclein occurs physiologically as a helically folded tetramer that resists aggregation. *Nature 477*, 107−123.
(33) Lee, J. C., Langen, R., Hummel, P. A., Gray, H. B., and Winker, J. R. (2004) α-Synuclein structures from fluorescence energy transfer kinetics: Implications for the role of the protein in Parkinson's disease. *Proc. Natl. Acad. Sci. U.S.A.*, 16466−16471.
(34) Yap, T. L., Gruschus, J. M., Velayati, A., Westbroek, W., Goldin, E., Moaven, N., Sidransky, E., and Lee, J. C. (2011) α-Synuclein interacts with glucocerebrosidase providing a molecular link between Parkinson and Gaucher diseases. *J. Biol. Chem. 286*, 28080−28088.
(35) Johnson, M., Coulton, A. T., Geeves, M. A., and Mulvihill, D. P. (2010) Targeted amino-terminal acetylation of recombinant proteins in *E. coli*. *PLoS One 5*, e15801.
(36) Maltsev, A. S., Ying, J., and Bax, A. (2012) Impact of N-terminal acetylation of α-synuclein on its random coil and lipid binding properties. *Biochemistry 51*, 5004−5013.
(37) Wang, C., Grey, M. J., and Palmer, A. G., III (2001) CPMG sequences with enhanced sensitivity to chemical exchange. *J. Biomol. NMR 4*, 361−366.
(38) Delaglio, F., Grzesiek, S., Vuister, G. W., Zhu, G., Pfeifer, J., and Bax, A. (1995) NMRPipe: a multidimensional spectral processing system based on UNIX pipes. *J. Biomol. NMR 6*, 277−293.
(39) Shen, Y., Delaglio, F., Cornilescu, G., and Bax, A. (2009) TALOS plus: A hybrid method for predicting protein backbone torsion angles from NMR chemical shifts. *J. Biomol. NMR 44*, 213−223.
(40) Biekofsky, R. R., Martin, S. R., Browne, J. P., Bayley, P. M., and Feeney, J. (1998) Ca^{2+} coordination to backbone carbonyl oxygen atoms in calmodulin and other EF-hand proteins: ^{15}N chemical shifts as probes for monitoring individual-site Ca^{2+} coordination. *Biochemistry 37*, 7617−7629.
(41) Schwieters, C. D., Kuszewski, J. J., Tjandra, N., and Clore, G. M. (2003) The Xplor-NIH NMR molecular structure determination package. *J. Magn. Reson. 160*, 65−73.
(42) Folmer, R. H., Hilbers, C. W., Konings, R. N., and Nilges, M. (1997) Floating stereospecific assignment revisited: Application to an 18 kDa protein and comparison with J-coupling data. *J. Biomol. NMR 9*, 245−258.
(43) Bermejo, G. A., Clore, G. M., and Schwieters, C. D. (2012) Smooth statistical torsion angle potential derived from a large conformational database via adaptive kernel density estimation improves the quality of NMR protein structures. *Protein Sci. 21*, 1824−1836.
(44) Hoeflich, K. P., and Ikura, M. (2002) Calmodulin in action: Diversity in target recognition and activation mechanisms. *Cell 108*, 739−742.
(45) Wishart, D. S., Bigam, C. G., Yao, J., Abildgaard, F., Dyson, H. J., Oldfield, E., Markley, J. L., and Sykes, B. D. (1995) H-1, C-13 AND N-15 Chemical-shift referencing in biomolecular NMR. *J. Biomol. NMR 6*, 135−140.
(46) Kang, L., Moriarty, G. M., Woods, L. A., Ashcroft, A. E., Radford, S. E., and Baum, J. (2012) N-terminal acetylation of α-synuclein induces increased transient helical propensity and decreased aggregation rates in the intrinsically disordered monomer. *Protein Sci. 21*, 911−917.
(47) Palmer, A. G., Kroenke, C. D., and Loria, J. P. (2001) NMR methods for quantifying microsecond-to-millisecond motions in biological macromolecules. *Methods Enzymol. 339*, 204−238.
(48) Holm, L., and Rosenström, P. (2010) Dali server: conservation mapping in 3D. *Nucleic Acids Res. 38*, 545−549.
(49) Fallon, J. L., Halling, D. B., Hamilton, S. L., and Quiocho, F. A. (2005) Structure of calmodulin bound to the hydrophobic IQ domain of the cardiac Ca(v)1.2 calcium channel. *Structure 13*, 1881−1886.
(50) Nagulapalli, M., Parigi, G., Yuan, J., Gsponer, J., Deraos, G., Bamm, V. V., Harauz, G., Matsoukas, J., de Planque, M. R. R., Gerothanassis, I. P., Babu, M. M., Luchinat, C., and Tzakos, A. G. (2012) Recognition pliability is coupled to structural heterogeneity: A calmodulin intrinsically disordered binding region complex. *Structure 20*, 522−533.
(51) Pfefferkorn, C. M., Heinrich, F., Sodt, A. J., Maltsev, A. S., Pastor, R. W., and Lee, J. C. (2012) Depth of α-synuclein in a bilayer determined by fluorescence, neutron reflectometry, and computation. *Biophys. J. 102*, 613−621.
(52) Wu, K.-P., Weinstock, D. S., Narayanan, C., Levy, R. M., and Baum, J. (2009) Structural reorganization of α-synuclein at low pH observed by NMR and REMD simulations. *J. Mol. Biol. 391*, 784−796.
(53) Bertoncini, C. W., Jung, Y.-S., Fernandez, C. O., Hoyer, W., Griesinger, C., Jovin, T. M., and Zweckstetter, M. (2005) Release of long-range tertiary interactions potentiates aggregation of natively unstructured α-synuclein. *Proc. Natl. Acad. Sci. U.S.A. 102*, 1430−1435.
(54) Irizarry, M. C., Kim, T. W., McNamara, M., Tanzi, R. E., George, J. M., Clayton, D. F., and Hyman, B. T. (1996) Characterization of the precursor protein of the non-Aβ component of senile plaques (NACP) in the human central nervous system. *J. Neuropath. Exp. Neur. 55*, 889−895.
(55) Rhoades, E., Ramlall, T. F., Webb, W. W., and Eliezer, D. (2006) Quantification of α-synuclein binding to lipid vesicles using fluorescence correlation spectroscopy. *Biophys. J. 90*, 4692−4700.
(56) Davidson, W. S., Jonas, A., Clayton, D. F., and George, J. M. (1998) Stabilization of α-synuclein secondary structure upon binding to synthetic membranes. *J. Biol. Chem. 273*, 9443−9449.

(57) DeWitt, D. C., and Rhoades, E. (2013) α-Synuclein can inhibit SNARE-mediated vesicle fusion through direct interactions with lipid bilayers. *Biochemistry 52*, 2385−2387.